



Contents lists available at ScienceDirect

Journal of the Mechanics and Physics of Solids

journal homepage: www.elsevier.com/locate/jmps

Skin and scales of teleost fish: Simple structure but high performance and multiple functions



Franck J. Vernerey^{a,*}, Francois Barthelat^b

^a Department of Civil, Environmental and Architectural Engineering, Program of Materials Science and Engineering, University of Colorado, Boulder, USA

^b Department of Mechanical Engineering, McGill University, Montreal, Canada

ARTICLE INFO

Article history:

Received 28 August 2013

Received in revised form

7 November 2013

Accepted 22 January 2014

Available online 26 March 2014

Keywords:

Biomaterials

Thin shells

Thin films

Structure-property relation

Modeling

ABSTRACT

Natural and man-made structural materials perform similar functions such as structural support or protection. Therefore they rely on the same types of properties: strength, robustness, lightweight. Nature can therefore provide a significant source of inspiration for new and alternative engineering designs. We report here some results regarding a very common, yet largely unknown, type of biological material: fish skin. Within a thin, flexible and lightweight layer, fish skins display a variety of strain stiffening and stabilizing mechanisms which promote multiple functions such as protection, robustness and swimming efficiency. We particularly discuss four important features pertaining to scaled skins: (a) a strongly elastic tensile behavior that is independent from the presence of rigid scales, (b) a compressive response that prevents buckling and wrinkling instabilities, which are usually predominant for thin membranes, (c) a bending response that displays nonlinear stiffening mechanisms arising from geometric constraints between neighboring scales and (d) a robust structure that preserves the above characteristics upon the loss or damage of structural elements. These important properties make fish skin an attractive model for the development of very thin and flexible armors and protective layers, especially when combined with the high penetration resistance of individual scales. Scaled structures inspired by fish skin could find applications in ultra-light and flexible armor systems, flexible electronics or the design of smart and adaptive morphing structures for aerospace vehicles.

© 2014 Elsevier Ltd. All rights reserved.

1. Introduction

Scaled skins are a very common structure in the animal kingdom: lizards, snakes, fish and even butterflies all possess a similar structure, which can however, significantly vary in size, morphology and function across species. The abundance of this structure generally is a hallmark of multifunctionality and ease of adaptation, a feature that is highly desirable in future generations of smart engineering materials. Fish skin is known for its remarkable mechanical properties: compliance, resistance to penetration (Yang et al., 2013a; Zhu et al., 2012a; Meyers et al., 2012; Zhu et al., 2012b; Vernerey and Barthelat 2010; Bruet et al., 2008) lightweight, all of them within an ultra-thin membrane structure. Despite these attractive features, this material has received little attention from the materials development community. In a review article on mineralized

* Corresponding author.

E-mail address: franck.vernerey@colorado.edu (F.J. Vernerey).

tissues, Currey noted that some fish scales are so tough that they could not be fractured “even after immersion in liquid nitrogen” (Currey, 1999). In a more recent study Ikoma et al (2003) characterized the structure of Pagrus Major (sea bream) and presented experimental data on the tensile behavior of a single scale, showing non-linearity and progressive failure, with a relatively high modulus (2.2 GPa) and tensile strength (90 MPa). Toughening mechanisms include pullout of mineralized collagen fibrils across cracks (Zhu et al., 2012b; Garrano et al., 2012; Yang et al., 2013b). For comparison, human skin, mostly composed of collagen has a modulus of 10–30 kPa (Pailler-Mattei et al., 2008) and a strength of 10 MPa (Silver et al., 2003). While the full range of the functions of this material is not known, it performs especially well in a variety of tasks. First of all, individual scales resist penetration and provide a physical barrier against predator attack (Yang et al., 2013a; Meyers et al., 2012; Bruet et al., 2008; Garrano et al., 2012; Zhu et al., 2013) in the form of, for instance, biting and puncture loads from other fish and marine birds. The intricate arrangement of the scales furthermore provides a flexible skin that possesses multiple mechanical functions. For instance, the skin has been shown to play a critical structural role in fish locomotion by regulating wave propagation (Long et al., 1996) and by acting as an external tendon (Hebrank and Hebrank, 1986; Hebrank, 1980) but also possessed inherent hydrodynamics properties (Sudo et al., 2002) that are crucial for swimming efficiency. These properties arise from a highly organized hierarchical structure, which is characterized by its simplicity, but nevertheless, as we report in this paper, which also display rich mechanical behavior and possess a high level of tunability, robustness and multifunctionality.

The macroscopic structure of scaled skin is reminiscent of the scaled armor used by ancient Roman military, to provide resistance to penetration while retaining relative freedom of movement. While such body armors share some mechanisms and duplicate some of the performance of natural fish scale, no systematic biomimetic “transfer of technology” was attempted so far because a fundamental understanding of the mechanics of fish skin is still lacking. The objective of this paper is thus to demonstrate, via a micromechanical model, that the mechanical interactions scales and dermis may, by themselves, be responsible for a number of features that are unique to fish scales. We particularly aim to show that when subjected to different modes of deformation including bending, stretch and compression, the skin displays a characteristic strain stiffening response and is able to resist bulking/wrinkling instabilities that are typical of such thin structures. Interestingly, the model points out the relative roles of mechanical factors influencing these responses; these include the properties of individual scales, the interactions between neighboring scales, as well as the behavior of the dermis and underlying tissues.

2. A simplified model to link fish skin structure and properties

In this study, we concentrate on the common leptoid scale type, which can be found on higher order bony fish and characterized by their arrangement in a head to tail direction, reminiscent of the structure of roof tiles (Jawad, 2005). As these scales greatly vary in shape, size and arrangement according to the fish, we propose here to develop a modeling approach that can be used to better understand the causality between structure and properties of fish skin. To compare model and experimental observations, we further propose to focus on four specific fish: the mullet (*Mugilidae*), the white perch (*Morone americana*), the striped bass (*Morone saxatilis*) and the milkfish (*Chanos chanos*), all distinguished by their similar, but different leptoid scales.

2.1. Structure of teleost fish skin

The skin of teleost fish can be thought of a soft asymmetric shell that comprises a highly elastic dermis on one side and a population of thin, but stiff scale on the other. The scale structure typically displays a quasi-periodic pattern comprised of alternate rows of overlapping scales running over the length of the fish (Fig. 1a and c). In the simplest description the scales can be characterized by their shape, size and overlapping distance (Fig. 1b and d) (Browning et al., 2013). Although size can significantly vary among species, we found that the normalized overlapping distance within a single row of scale is remarkably consistent. For instance, for the four fish considered in this study, the ratio r of the scale spacing to the length of a single scale was comprised between $r=0.2$ for the milkfish and $r=0.3$ for the mullet (Fig. 1c and d). Striped bass and the white perch displayed intermediate configurations with $r=0.25$. Individual scales are attached to the underlying dermis by small pockets of skin, which overlap approximately half of the scale length (Fig. 1d). These pockets are characterized by an intricate net-like structure supported by a soft elastic film (the dermis) that gives the skin its high deformability. More importantly, these pockets function as elastic sleeves for individual scales (Fig. 1d) providing resistance to their out-of-plane rotation as the overall skin bends. The scales themselves are characterized by an elastic modulus that is several orders of magnitude larger than the dermis (Zhu et al., 2013). Meanwhile, their small thickness ensures a finite bending rigidity and low weight. Overall, the interactions between the scales and the underlying dermis offer a variety of mechanical functions that are essential to fish survivability, such as freedom of motion, swimming efficiency, lightweight, robustness, protection and escape mechanism. For instance, recent studies on artificial (Browning et al., 2013) and natural scale (Zhu et al., 2013) have shown that the interaction between scales plays a significant role to resist sharp puncture.

To first investigate the role of scales on skin bending, we first designed a simple pinching test in which a skin specimen (with scales) is removed from the fish body and immediately subjected to a force-couple (with forceps) which induced large skin curvature (Fig. 2a). This strategy ensured that the skin remained fully hydrated during the test but did not allow a direct measurement of the force–displacement relation. This test was however particularly useful to understand the synergy

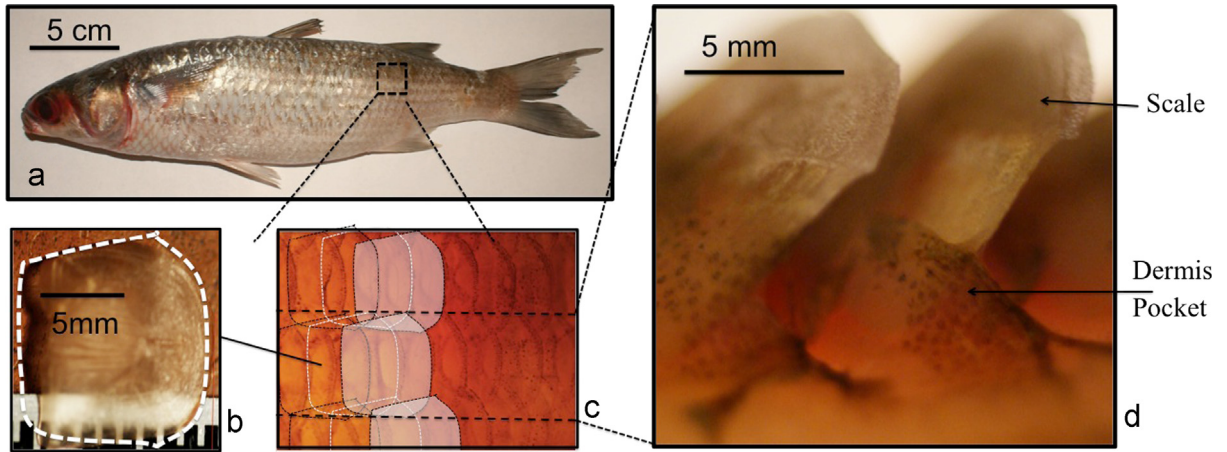


Fig. 1. A multiscale view of the scaled skin of the mullet. (a) Overall fish physiognomy, (b–c) close-up of a scale and their arrangement into an alternate, periodic pattern, and (d) magnification of a single layer of scales displaying the scale overlap and their connection with the underlying dermis, and in particular, the pocket providing scales with a rotational stiffness.

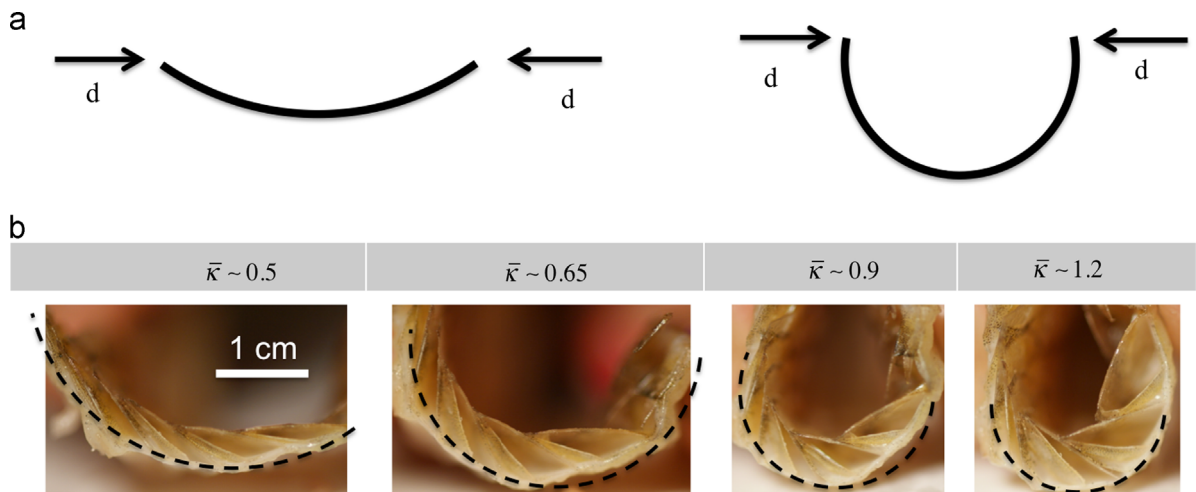


Fig. 2. (a) Pinching experiment to apply large bending deformations to fish skin and (b) observation of the scales rotation during skin bending. The normalized bending curvature $\bar{\kappa}$ is also shown in each configuration.

between scale and dermis deformation during bending, as shown in Fig. 2. For concave bending (scales are on the inside of the curve), Fig. 2b clearly shows that skin bending involves a significant rotation of individual scales, a feature that is associated with a rise on the skin's bending resistance with curvature. On the other hand, for convex bending the scales play no role in the skin mechanics and the structure remains extremely soft.

2.2. A micromechanical model to relate structure and mechanical response

In order to facilitate the development of models and to unveil new mechanisms and features, we idealized the scaled skin as a one-dimensional substrate layer onto which a regular arrangement of scales of length l separated by a distance $s=rl$ is attached (Fig. 3a). In this simplified model we assume that the scales are homogenous. While more elaborate computational models of the full three-dimensional structure can be found in the literature (Vernerey et al., 2014), such simplified analytical models are powerful at extracting the essence of fish skin mechanics without relying on computationally expensive computational techniques. Mechanically, the scales are characterized by a bending stiffness EI , with E Young's modulus of the scales and I their moment of inertia. Meanwhile, the scale pockets are represented by linear angular springs of stiffness K at the base of each scale. Indeed, scale rotation induces the opening of the dermis pocket, which may undergo significant stretch as can be seen in Fig. 1d. Since this deformation effectively resists scale rotation, it can be considered as a rotational spring. For natural fish skins, the stiffness of the dermis pocket is relatively low compared to that of the scale; this implies that K is expected to be significantly smaller than the effective bending stiffness $(EI)_b/\ell$ of the scales.

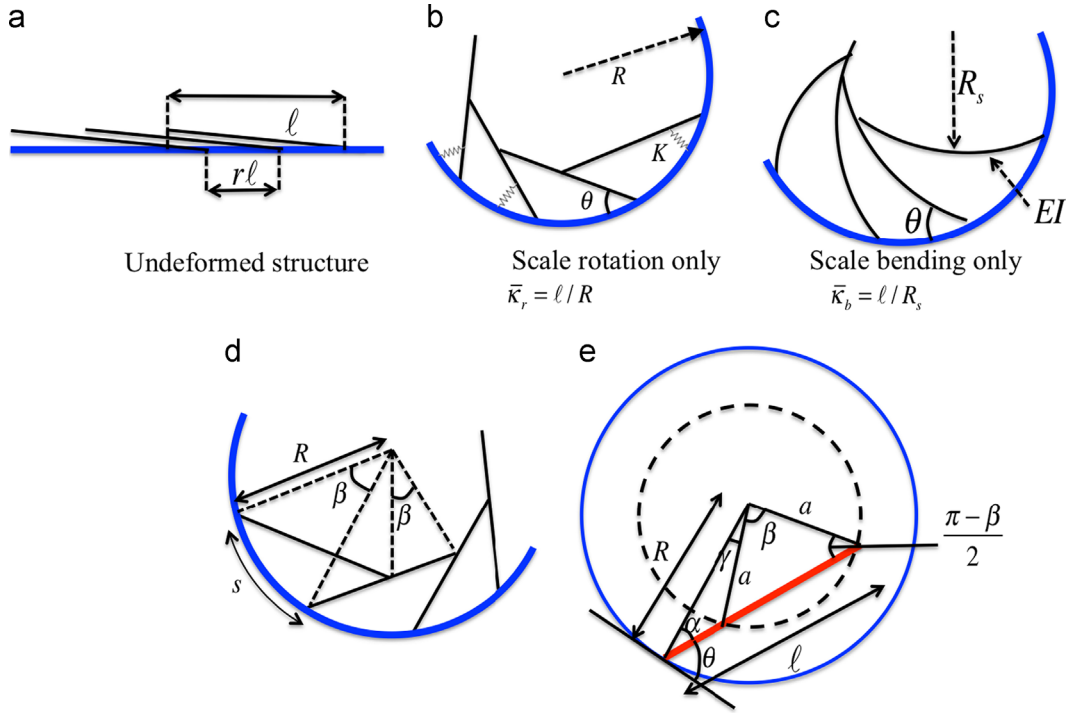


Fig. 3. (a) One-dimensional representation of the fish scale structure in its undeformed configuration and decomposition of the skin curvature into (b) a curvature κ_r associated with scale rotation only and (c) a skin curvature κ_b with scale bending only. Schematics (d) and (e) introduce the relevant geometric variables to build the model. (For interpretation of the references to color in this figure, the reader is referred to the web version of this article.)

The overall bending of the structure (on the concave side) can then be conveniently described in terms of the normalized curvature $\bar{\kappa} = \ell/R$ where R is the radius of curvature as shown in Fig. 2b.

2.2.1. Relationship between scale rotation and skin curvature

For simplicity, we assume that scales are beams that undergo a homogeneous bending deformation (curvature κ_b) and rotate with angle θ with respect to the dermis. To characterize the mechanics of the system, we first determine the relationship between the overall concave curvature $\bar{\kappa}$, the scale rotation θ and the normalized scale curvature $\bar{\kappa}_b$ from geometrical arguments. For this, it is first convenient to introduce a so-called “rotation-induced curvature” $\bar{\kappa}_r$ defined as the curvature $\bar{\kappa}$ that would be measured if the scales were to rotate without bending (Fig. 3b). Under the assumption of small to moderate scale bending ($\bar{\kappa}_b < 0.1$), it is acceptable to additively decompose the total curvature into a component driven by scale bending and a component driven by scale rotation as follows:

$$\bar{\kappa} = \bar{\kappa}_r + \bar{\kappa}_b \tag{1}$$

This decomposition will be particularly useful to understand the relative contributions of dermis pockets (driving scale rotation) and scale stiffness (driving scale bending) in the overall response of the skin.

To compute the relationship between the scale rotation angle θ and the rotation curvature $\bar{\kappa}_r$, we consider that the flexural deformation of each scale is small enough that it does not affect the computation of scale rotation. This assumption has been shown to be quite accurate by numerical models, for instance in Vernerey and Barthelat (2010). In this context, we consider an assembly of rotated scales, represented as straight segments as shown in Fig. 3a. We then consider the triangles shown in Fig. 3b in which a single scale (in red) is shown to lie in between a large circle of radius R (point of attachment) and a small circle of radius a (tip of the scale). Relevant angles α , β , γ and θ are shown in the figure. Applying the law of sines to the appropriate triangles leads to

$$\frac{\sin(\alpha)}{a} = \frac{\sin((\pi-\beta)/2)}{R} = \frac{\sin(\gamma+\beta)}{l} \tag{2}$$

where angle γ is related to β and α by $\gamma = \frac{\pi}{2} - \frac{\beta}{2} - \alpha$. Substituting this expression and rewriting the last equality of (2) yields

$$\bar{\kappa}_r \cos(\beta/2) = \cos(\beta/2 - \alpha). \tag{3}$$

Subsequently using $\theta = \frac{\pi}{2} - \alpha$, we obtain an equation for θ

$$\bar{\kappa}_r \cos(\beta/2) = \sin(\beta/2 + \theta), \quad \text{which implies that} \quad \theta = -\frac{\beta}{2} + \sin^{-1}\left(\bar{\kappa}_r \cos\left(\frac{\beta}{2}\right)\right). \tag{4}$$

Now invoking Fig. 3a, one can deduce that angle β is related to the relative curvature and the ratio $r = s/\ell$ of the scale spacing and length by $\beta = s/R = r\bar{\kappa}$. Using this relationship in Eq. (4) leads to the targeted relationship between scale rotation and overall skin curvature:

$$\theta(\bar{\kappa}_r) = -\frac{r\bar{\kappa}_r}{2} + \sin^{-1}\left(\bar{\kappa}_r \cos\left(\frac{r\bar{\kappa}_r}{2}\right)\right). \quad (5)$$

As shown in Fig. 2b, the bending of the scales (measured by curvature κ_b) can then be computed by the difference between the general and the rotation-induced curvature from (1):

$$\bar{\kappa}_b = \bar{\kappa} - \bar{\kappa}_r \quad (6)$$

Note: As mentioned above, our kinematic analysis is only valid for small to moderate scale bending ($\bar{\kappa}_b < 0.1$) but remains true for very large values of scale rotation. This assumption that is valid for a majority of fish-skins; for instance, in Fig. 2, it can be observed that the bending of individual scales remains relatively small, even for very large skin curvatures. For cases in which scale bending becomes large, more advanced computational methods may be used as introduced in Vernerey and Barthelat (2010) and Vernerey et al. (2014).

2.2.2. Mechanical response of fish skins

We now seek to derive a relationship between the internal moment M and the total curvature κ based on the detailed micromechanics of fish skin deformation. Considering an energetic approach, we use that fact that the elastic energy stored in the entire structure is equal to the cumulative contribution of the stored energy in each component of the assembly (scale and attachment). From a micromechanics point of view, the elastic energy E stored in the fish skin per unit length s (the scale spacing) is then

$$E = \frac{l}{s}E_b(\bar{\kappa}_b) + E_r(\theta(\bar{\kappa}_r)) \quad (7)$$

where E_b is the energy stored due to scale bending, E_r is the elastic energy stored in the scale pocket due to scale rotation θ and $\ell/s = 1/r$. Assuming here that the scales and the angular spring behave in a linear elastic fashion and normalizing the energies by the quantity $(EI)_s/r\ell$, one can write a normalized energy \bar{E} in the form:

$$\bar{E} = \bar{E}_b(\bar{\kappa}_b) + \bar{E}_r(\theta) \quad \text{where} \quad \begin{cases} \bar{E}_b(\bar{\kappa}_b) = 1/2\bar{\kappa}_b^2 \\ \bar{E}_r(\theta) = 1/2\bar{\kappa}\theta^2 \end{cases} \quad (8)$$

where the normalized stiffness measures are given by $\overline{(EI)}_b = 1$ and $\bar{K} = K/\ell(EI)_b$ while all curvatures are normalized by the length ℓ (or $\kappa = \kappa\ell$). Here, we introduced K as the stiffness of the angular spring representing an effective measure of the “scale pocket” property. To compute the mechanical response of the skin, we now invoke the principle of energy minimization by stating that for a given macroscopic curvature $\bar{\kappa}$, the decomposition of the deformation into scale rotation ($\bar{\kappa}_r$) and scale bending ($\bar{\kappa}_b$) is such that the stored energy \bar{E} satisfies:

$$\left. \frac{\partial \bar{E}}{\partial \bar{\kappa}_r} \right|_{\bar{\kappa}} = - \left. \frac{\partial \bar{E}}{\partial \bar{\kappa}_b} \right|_{\bar{\kappa}} = 0, \quad \text{which is equivalent to} \quad \frac{\partial \bar{E}_r}{\partial \theta} \frac{\partial \theta}{\partial \bar{\kappa}_r} - \frac{\partial \bar{E}_b}{\partial \bar{\kappa}_b} = 0. \quad (9)$$

Using Eq. (8), one gets $\partial \bar{E}_b / \partial \bar{\kappa}_b = \bar{\kappa}_b$ and $\partial \bar{E}_r / \partial \theta = \bar{K}\theta$ and invoking the equality $\bar{\kappa} = \bar{\kappa}_b + \bar{\kappa}_r$, we finally obtain the following nonlinear equation for $\bar{\kappa}_r$:

$$\bar{\kappa}_r + \bar{\kappa}\theta(\bar{\kappa}_r)\theta'(\bar{\kappa}_r) = \bar{\kappa} \quad (10)$$

where the expression for θ and its derivative $\theta' = \partial\theta/\partial\bar{\kappa}_r$ are explicit functions of $\bar{\kappa}_r$ as seen in (5) and in the following expression obtained from (5):

$$\theta'(\bar{\kappa}_r) = -\frac{r}{2} + \frac{\cos(r\bar{\kappa}_r/2) - (r\bar{\kappa}_r/2)\sin(r\bar{\kappa}_r/2)}{\sqrt{1 - (\bar{\kappa}_r \cos(r\bar{\kappa}_r/2))^2}}. \quad (11)$$

For a given value $\bar{\kappa}$, it is therefore possible to find the value of $\bar{\kappa}_r$ numerically using a nonlinear Newton–Raphson solver. The relationship between the overall internal moment M and the curvature $\bar{\kappa}$ is then obtained by computing the derivative of the energy \bar{E} with respect to the total curvature $\bar{\kappa}$ as

$$\bar{M} = \frac{\partial \bar{E}}{\partial \bar{\kappa}} = \bar{\kappa}_b \quad (12)$$

where $\bar{\kappa}_b = \bar{\kappa} - \bar{\kappa}_r$. Rewriting the same equation in dimensional form, we obtain:

$$M(\kappa) = \frac{(EI)_s}{r\ell}(\bar{\kappa} - \bar{\kappa}_r(\kappa)). \quad (13)$$

We note that while the value of the spring stiffness K does not explicitly appear in the above equation, its influence is clear since the value of $\bar{\kappa}_r$ is the solution of (10) which is, itself, an explicit function of K . Eq. (13) is important as it enables

the investigation of the moment-curvature response of the fish skin for a variety of geometrical (r, ℓ) and material parameters ($(EI)_d, (EI)_s, K$) as shown below.

Before the model is used to investigate the behavior of the skin, we wish to provide a discussion of its assumptions, limitations and possible improvements. First of all, the above study is based on a 1D arrangement of scales and ignores their 2D staggered arrangement. Consequently, the model can only predict the skin behavior in the head-to-tail (or longitudinal) direction and may underestimate the true stiffness of the 2D skin. In this context, a full 2D model, relying on numerical methods can be used (readers are directed to our previous work in Vernerey et al. (2014)), although its apparent complexity may be an obstacle to understand the most fundamental micromechanics of fish-skins. Second, it is clear that our model only accounts for the stiffness of the scale layer, without accounting for the presence of the underlying, elastic dermis. In fact, if one notes that scales and dermis are two parallel components of the entire skin, it can be deduced that the overall stiffness is simply the sum of each of the component's stiffness, assuming that the neutral axis is located on the dermis. The predicted behaviors discussed in the following section can therefore be thought of as an added contribution to the response of the dermis only.

3. Investigation of the mechanical response of fish skin

In this section, we propose to use the above model to investigate the properties of single fish scales (both geometrical and mechanical) on the overall response of the skin. We particularly aim to explore three key features of fish skin: (a) response to bending deformation, (b) response to in-plane stretch, (c) response to in-plane compression and (d) robustness, i.e., its capacity to preserve its unique mechanical behavior upon damage.

3.1. Response in bending: a strain-stiffening shell.

Because fish-skin is an asymmetric (it is made of a dissimilar structure on the outer and inner sides), it is differently affected by concave and convex bending. For convex bending, scales are on the external side of the curve and are thus incapable of interacting with the dermis. As a result, the overall bending stiffness of the skin is that of the soft dermis. More interestingly, when concave bending occurs, the response is driven by the presence of scales, for which the moment-curvature relationship is shown in (13). In this situation, the model generally shows that the rotational stiffness of the skin pocket plays a large role in the overall response of the material, ranging from linear to strongly nonlinear depending on the value of \bar{K} (Fig. 4a). For high pocket stiffness, scale bending is the preferred mode of deformation and the moment-curvature response becomes essentially linear with a stiffness EI/r that is determined by the individual rigidity of scales and their density $1/r$. When the pocket stiffness decreases, the elastic response transitions to a very nonlinear “bending stiffening” behavior that is eventually dominated by scale rotation. For low values of \bar{K} (below 0.05 in Fig. 4a), small bending regimes exclusively involve scale rotation, which results in a low bending stiffness of the skin. For intermediate curvatures, stiffening is observed as scale rotation becomes increasingly harder due to geometrical constraints. For high curvatures ($\bar{\kappa} \sim 1$), a phenomenon interpreted as “scale locking” precludes any additional rotation; this ultimately results in a deformation regime dominated by scale bending and its associated high stiffness. Interestingly, the model predicts in these conditions, the skin stiffness converges to that of individual scale (EI/r). In other words, from a sharp indenter's perspective, the skin behaves like rigid body armor whose protective capacity is that of a pile of stacked scales. It has been shown in previous studies (Zhu et al., 2013) that such a pile is indeed excellent at resisting indentation. In another context, comparisons of experimental observations (Fig. 2a) and model simulations (Fig. 4a) suggest that pocket stiffness is small compared to scale stiffness ($\bar{K} \ll 1$) which corresponds to significant bending stiffening of the structure. To further investigate the effect of scale overlap r on the skin mechanics, we performed a numerical study that quantified the normalized stiffness

$$\bar{\beta} = \frac{r\beta}{(EI)_s}. \quad (14)$$

where β is the bending stiffness of the skin at zero curvature. Results depicted in Fig. 4b also suggest a weak dependency of $\bar{\beta}$ on r , implying that the stiffening behavior of the skin is inherent to the scaled structure, regardless of its arrangement (as long as $r < 1$). In analogy to most biological materials known for their strain stiffening response, scaled skins provide a unique solution that combines both strain and flexural stiffening capabilities. This characteristic may be crucial for many functions as shown in Fig. 4c. The low stiffness at low curvature is indeed a requirement for freedom of motion. The intermediate stiffening responses possesses the elastic characteristic of an external tendon that restitutes mechanical energy and optimizes efficiency during swimming (Long et al., 1996). Finally, the situation in which $\bar{\kappa}$ is close to unity involves extreme curvatures that may originate from the indentation of a sharp indenter (during a predator's bite for instance (Meyers et al., 2012; Zhu et al., 2013)). In this case, the skin behaves like a penetration resistant shell.

3.2. Response in stretch: a soft elastic skin

Another important modes of skin deformation, which is relevant to fish swimming, is in-plane stretch. For the type of fish considered here, the skin stretches elastically to large strains (around 50% as seen in Fig. 5) and the mechanisms involved (in tension) are independent from the presence of scales. The friction between the scales is negligible (Zhu et al., 2013) so that they freely slide on the skin as it stretches (Fig. 5). The high elasticity of the structure may play a significant

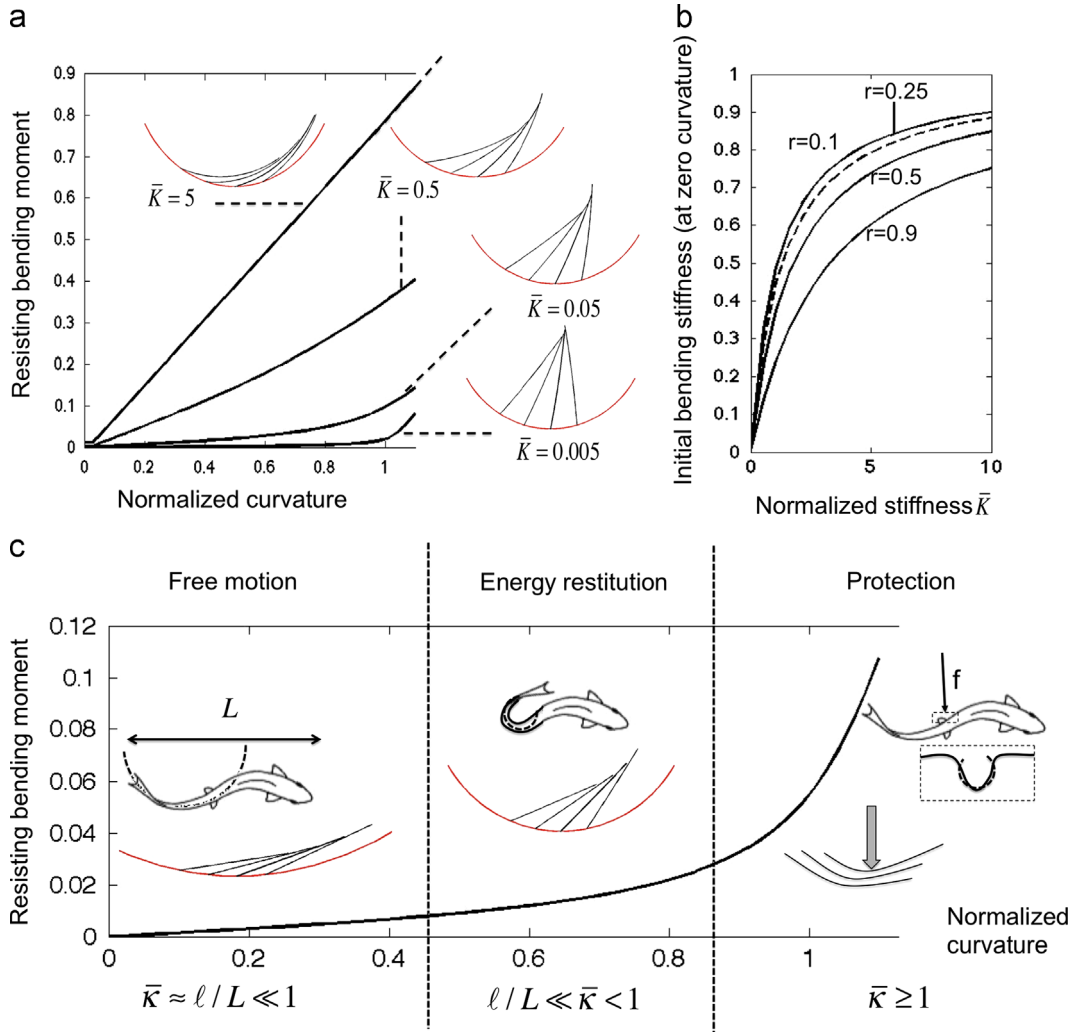


Fig. 4. Role of scale and attachment stiffness on the overall deformation mechanism. (a) Effect of the relative dermis pocket stiffness \bar{K} on the normalized moment-curvature ($\bar{M}/\bar{\kappa}$) response of the structure (for a scale overlap $r=0.25$). (b) Normalized Initial bending stiffness $\bar{\beta}$ (Eq. 14) as a function of \bar{K} for different value of scale overlap. (c) Different fish skin bending regimes and their possible functions on fish swimming and protection.

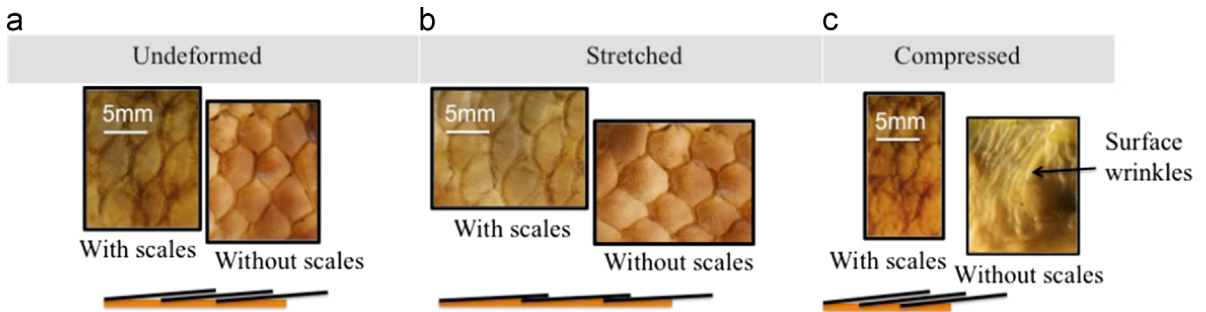


Fig. 5. Deformation modes of the scaled structure. (a) Undeformed fish skin with and without scales. (b) Stretch: larger strains are possible due to scale sliding and the low stiffness of the underlying dermis. (c) Compression: the presence of scales prevents instability mechanisms such as wrinkling and buckling of the dermis.

energy-restituting role during swimming. Indeed, fish bending during swimming involves significant stretch of the skin on the convex side of the curvature. The elastic response ensures that the curvatures remain fairly uniform while the skin can store enough mechanical energy to efficiently help the next stride.

3.3. Response in compression: a buckling-proof membrane

In contrast, the compression regime is largely dependent on the presence of scales, which plays an essential role in stabilizing the material (Fig. 5c). Indeed, similar to a majority of thin films and membranes, the dermis alone cannot sustain large compressive loads due to the early appearance of mechanical instabilities in the form of buckling and wrinkling (Fig. 5c). When scales are present, however, in-plane compressive strains can be sustained up to unusual levels (~100% as seen in Fig. 5c). To better understand this phenomenon, it is useful to consider a strip of skin (with scales) with initial length L_0 , that is subjected to a compressive stress σ and rotation constraints as illustrated in Fig. 6. The deformation of the strip, described by the linear strain $\varepsilon = 1 - L/L_0$ subsequently induces a change in scale overlap such that the overlap ratio becomes $r = (1 - \varepsilon)r_0$, r_0 being the overlap ratio before deformation. For a freestanding asymmetric shell (or beam), the critical buckling stress is dependent on the bending direction (concave or convex). If bending occurs on the convex side, the presence of scales is not felt and the critical buckling stress is determined by Euler's formula as: $\sigma_d = \pi^2(EI)_d/(AL^2)$, A being the cross-sectional area of the dermis layer. In most situations, however, the skin is supported by an underlying substrate and buckling is restricted to the concave side of the skin. In this case, Euler's formula is affected by the presence of scales and the critical buckling stress σ_c takes the form

$$\sigma_c = \sigma_d \left(1 + \frac{\beta(r)}{(EI)_d} \right) = \sigma_d \left(1 + \frac{(EI)_s \bar{\beta}(r)}{(EI)_d r} \right) \quad \text{where } r = (1 - \varepsilon)r_0 \quad (15)$$

where the first term refers to the contribution of the dermis layer, the second refers to the contribution of the scales while the quantity $\beta(r)$ is the initial bending stiffness of the scale assembly shown in Fig. 4b. We also note that the right-hand side of (15), obtained with the help of Eq. (14), clearly shows that σ_c is a function of the compressive strain through the overlap ratio r . Indeed, as the skin is compressed, scale overlap increases (Fig. 5c) and so does the critical buckling stress. To assess the conditions for skin buckling, we then write the compressive stress/strain relationship in the form $\sigma = E\varepsilon$ where E is Young's modulus of the dermis. When normalized with respect to the buckling stress σ_d of the dermis, this relation becomes:

$$\bar{\sigma} = \frac{12}{\pi^2} \left(\frac{L}{t_d} \right) \varepsilon. \quad (16)$$

where t_d is the thickness of the dermis layer and we used the fact its area moment of inertia is $I = wt_d^3/12$, with w the width of the strip. Fig. 6 shows how the normalized buckling stress (in log scale) increases with normalized pocket stiffness \bar{K} and strain. For small or vanishing values of \bar{K} , one can see that the applied stress eventually reaches a critical value at which buckling occurs. However, as \bar{K} becomes closer to unity, the buckling stress of the skin σ_c becomes two to three order of magnitudes larger than the buckling stress σ_d of the dermis. When this occurs, it can be seen in Fig. 6 that the buckling strain (given by the intersection of solid and dotted lines) becomes increasingly large. This phenomenon clearly explains why large compressive strains can be applied to a scaled skin without buckling, as depicted in Fig. 5c.

Together, these results suggest that the pocket stiffness \bar{K} plays a significant role in resisting out-of-plane scale rotation and thus postponing the critical buckling load of the skin. This stabilization mechanism becomes even more preponderant with strain as the decreasing scale-to-scale distance contributes to stiffening the structure. This mechanism may be of importance during fish swimming as the overall bending of the fish body results in strong compressive forces in the concave regions. Because of the absence of wrinkling, the skin can bear significant loads and efficiently restitutes elastic energy.

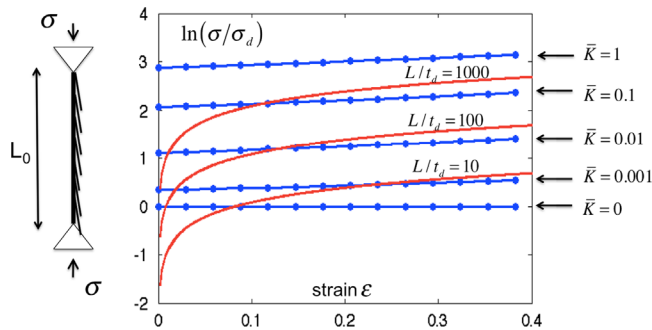


Fig. 6. Buckling analysis of fish skin. The dotted lines show how the normalized buckling stress $\bar{\sigma}_c = \sigma_c/\sigma_d$ (in a log scale) increases with the normalized pocket stiffness \bar{K} . The continuous (red) lines show the corresponding normalized stress–strain curves (Eq. 16) for three different ratios of the skin length ad dermis thickness. The buckling strains in different situations can be visualized as the intersection of the dotted and solid lines. In these results, the ratio $(EI)_s/(EI)_d$ appearing in (15) was taken to be 1000 according to values reported in the literature for dermis modulus (Pailler-Mattei et al., 2008), scale modulus (2.2 GPa) and a ratio of dermis to scale stiffness of 10 (our observations). (For interpretation of the references to color in this figure legend, the reader is referred to the web version of this article.)

3.4. Robustness of the mechanical response: a material that enables escape mechanisms and lightweight

A particular feature of scale/dermis interaction is the ease by which scales rub off when a force is applied tangentially to the scale in a direction pointing toward the back of the fish (Fig. 7a). Such deciduous scales (Benoit et al., 2012) are key to fish survivability as they enable fast escape by abandoning scales soon after a fish is grasped by potential predators. Under clamping-type forces resulting from a predator’s bite (which may be distributed on one or more scales), it is reasonable to hypothesize that skin protection relies on two mechanisms: (a) mechanical resistance to the biting force by energy dispersion (Vernerey and Barthelat 2010) and dissipation (Bruet et al., 2008) and (b) scale loss, which helps the prey escape from its predator’s grip. Therefore, considering scale removal as an intrinsic response of fish skin, it is possible to characterize the robustness of the material by measuring how its protective and mechanical functions are affected by the removal of one or more scales. It has been shown above that these functions all depend on the concept of scale overlap; in other words, the performance of the skin decreases when scales no longer overlap ($r > 1$). This is particularly true for the bending stiffening response which is little sensitive to the ratio r as shown in Fig. 4b but strongly dependent on scale overlap. A measure of robustness may thus be introduced by an integer η that indicates the maximum number of scales that can be removed before scales cease to overlap. It is straightforward to show that η is a discontinuous function of the scale spacing r of the form:

$$\eta(r) = i - 1 \quad \text{with} \quad \frac{1}{i+1} \leq r < \frac{1}{i} \quad \text{and} \quad i = 1, \dots, n \quad (17)$$

For instance, the case $i=1$ corresponds to the case where r lies between $1/2$ and 1 . In this case, the removal of one scale results in a non-overlapping scale structure and the robustness is $\eta(r) = 0$. The robustness therefore increases as r decreases, or in other words when the number of scales per unit area of skin increases at the expense of lightweight. To demonstrate the influence of scale density on mass, we first consider that, regardless of scale arrangement, the ultimate stiffness of the skin is constrained to reach the steady value given by $K^* = EI/r$ to preserve its protection capabilities. Considering the case of rectangular scales with thickness h , width b and bending moment of inertia $I = bh^3/12$, one can easily find a relationship between the thickness of a scale and the overlap factor as $h = (12K^*r/(Eb))^{1/3}$. Further noticing that the mass density of the skin (per unit area) is given by $\rho = \bar{\rho}bh/r$ where $\bar{\rho}$ is the mass density (per unit volume) of the scale, we can derive the following relationship between mass density ρ and ratio r :

$$\rho = \alpha \left(\frac{b}{r}\right)^{2/3} \quad \text{where} \quad \alpha = \bar{\rho} \left(\frac{12K^*}{E}\right)^{1/3} \quad (18)$$

In other words, similarly to robustness, the mass density increases with scale density. Based on the hypothesis that the natural design of fish skin tends to maximize its robustness while minimizing its mass density, an optimal value of the relative spacing r can be calculated. As shown in Fig. 7, it is possible to create an objective function in the form

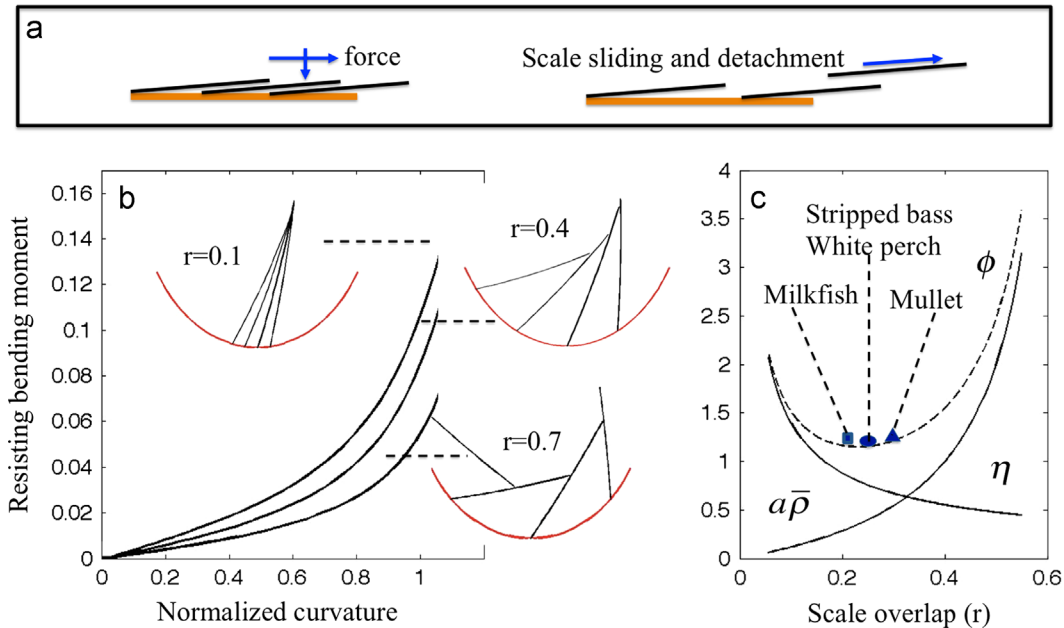


Fig. 7. The competition between Robustness and weight in fish structures. (a) Schematic of the scenario leading to scale detachment. A combination of normal and tangential forces is applied on a scale in a head to tail direction, eventually leading to its disconnection from the dermis pocket. (b) Role of scale overlap on the stiffening response of the skin (for $\bar{K} = 0.02$). (c) Variation of robustness and weight with overlap ratio. The diagram shows that a compromise between low weight and acceptable robustness occurs when r is between 0.2 and 0.3, values that are in good agreement with observed values.

$f(r) = \rho(r) + a/\eta(r)$, where a is a constant which upon minimization, yields an optimum value of r . A realistic value of the constant a can be chosen such that mass and robustness are weighted appropriately. For instance, a choice of $a = 0.3(ab^{2/3})$ leads to the function depicted in Fig. 7c, yielding a value $r \sim 0.25$. This value ensures that two or three scales can be removed from the structure without significantly affecting its function, while remaining very light. This finding matches particularly well the values measured on the four fish investigated as part of this study as shown in Fig. 6. Overall, these results suggest that despite its variation among fish species, fish skin has evolved to promote escape mechanisms (via scale detachment) while optimizing robustness and lightweight. Robustness is indeed a large player in survivability, especially in fish that are “low in the food chain”. Interesting future studies could study the relationship between the structure of skin of fish in different environment (aggressive predators, strong currents etc.). For example a fish on top of the food chain would probably favor lightweight over robustness and vice-versa.

4. Concluding remarks

As a summary, we showed through experimental observations and simple modeling demonstrations that despite its simple structure, the scaled structure of fish skin displays a very rich and adaptable behavior. Within a thin, flexible and lightweight layer, the structure displays a variety of strain stiffening and stabilizing mechanisms which promote various functions such as protection, robustness and swimming efficiency. We have particularly highlighted three key important features pertaining to the mechanical behavior of scaled skins. First, the tensile behavior of the skin displays a highly elastic behavior which is independent from the presence of rigid scales. More important though, was the behavior of the skin during compression, for which the interaction between scales and dermis precluded the appearance of buckling and wrinkling instabilities, which are usually predominant for thin membranes. While the biological functions for this behavior are not clear, the replication of these mechanisms in thin, flexible engineering materials such as flexible electronics is surely desirable. The second result of this paper pertains to the bending response of fish skins. We report here that scaled-skins provides unique mechanisms to achieve strain stiffening in bending while preserving a very small thickness. This nonlinear behavior originates from purely geometric constraints between neighboring scales, which can be easily tuned by changing the properties and geometry of the dermis pockets holding the scales. Besides the simplicity of the mechanisms at play, the curvature stiffening capacity of the skin is likely to play a significant biological role in fish swimming and in resistance against puncture loads that results from predator attacks. In this respect, fish scales consist of a very interesting model for the development of very thin and flexible armors and protective layers, especially when combined with high penetration resistance of individual scales (Zhu et al., 2012b). Third and last, this paper has demonstrated that fish skin is a very robust material that preserves its key mechanical characteristics despite the presence of structural defects that can be the removal or rupture of individual scales. Observation of the scale overlap in four types of fish even suggests that fish skin tends to maximize robustness and minimize weight. Overall, the scaled structure of fish skin is an intriguing membrane system that displays a rich spectrum of mechanical responses due to a subtle arrangement of building blocks (scale, dermis, pockets) and that is highly adaptable as a function of specific biological functions (such as external tendon and armor protection). The domain of applications of scaled structures could span many engineering applications, from ultra-light and flexible armor systems to important future technological development including flexible electronics or the design of smart and adaptive morphing structures for aerospace vehicles. Many key research and technology advances may therefore be positively affected by a stronger effort in the study of this material system.

Acknowledgment

The authors wish to acknowledge the support of the US National Science Foundation, program of Nano and biomechanics, under award 0927585.

References

- Benoit, H.P., Plante, S., Kroiz, M., Hurlbut, T., 2012. A comparative analysis of marine fish species susceptibilities to discard mortality: effects of environmental factors, individual traits, and phylogeny. *ICES J. Mar. Sci.* 70 (1), 99–113. (Aug).
- Browning, A., Ortiz, C., Boyce, M.C., 2013. Mechanics of composite elasmoid fish scale assemblies and their bioinspired analogues. *J. Mech. Behav. Biomed. Mater.* 19, 75–86.
- Bruet, B.J.F., Song, J., Boyce, M.C., Ortiz, C., 2008. Materials design principles of ancient fish armour. *Nat. Mater.* 7 (9), 748–756. (September).
- Currey, J.D., 1999. The design of mineralised hard tissues for their mechanical functions. *J. Exp. Biol.* 202 (23), 3285–3294.
- Garrano, A., Marino Cugno, La Rosa, G., Zhang, D., Niu, L.N., Tay, F.R., Majd, H., Arola, D., 2012. On the mechanical behavior of scales from *Cyprinus carpio*. *J. Mech. Behav. Biomed. Mater.* 7, 17–29.
- Hebrank, J.H., Hebrank, M.R., 1986. The mechanics of fish skin – lack of an external tendon role in two teleosts. *Biol. Bull.* 171 (1), 58–68.
- Hebrank, M.R., 1980. Mechanical properties and locomotor functions of eel skin. *Biol. Bull.* 158, 58–68.
- Ikoma, T., Kobayashi, H., Tanaka, J., Walsh, D., Mann, S., et al., 2003. Physical properties of type I collagen extracted from fish scales of *Pagrus major* and *Oreochromis niloticus*. *Int. J. Biol. Macromol.* 32 (3–5), 199–204. (September).
- Jawad, L.A., 2005. Comparative morphology of scales of four teleost fishes from Sudan and Yemen. *J. Nat. Hist.* 39 (28), 2643–2660.
- Long, J.H., Hale, M.E., Henry, M.J.M.C., Westneat, M.W., 1996. Functions of fishskin: flexural stiffness and steady swimming of longnose gar *Lepisosteus osseus* 2151, 2139–2151.
- Meyers, M.A., Lin, Y.S., Olevsky, E.A., Chen, P.-Y., 2012. Battle in the Amazon: *Arapaima* versus *Piranha*. *Adv. Eng. Mater.* 14, B279–B288.

- Pailler-Mattei, C., Bec, S., Zahouani, H., 2008. *in vivo* measurements of the elastic mechanical properties of human skin by indentation tests. *Med. Eng. Phys.* 30 (5), 599–606. (June).
- Silver, F.H., Siperko, L.M., Seehra, G.P., 2003. Review mechanobiology of force transduction in dermal tissue. *Skin Res. Technol.* 3–23.
- Sudo, S., Tsuyuki, K., Ito, Y., Ikohagi, T., 2002. A study on the surface shape of fish scales. *JSME Int. J. Ser. C-Mech. Syst. Mach. Elem. Manuf.* 45 (4), 1100–1105.
- Vernerey, F.J., Barthelat, F., 2010. On the mechanics of fishscale structures. *Int. J. Solids Struct.* 47 (17), 2268–2275. (August).
- Vernerey, F.J., Musiket, K., Barthelat, F., 2014. Mechanics of fish skin: a computational approach for bio-inspired flexible composites. *Int. J. Solid Struct.* 5 (1), 274–283.
- Yang, W., Chen, I.H., Gludovatz, B.Z., Zimmerman, E.A., Ritchie, R.O., Meyers, M.A., 2013a. Natural flexible dermal armor. *Adv. Mater.* 25, 31–48.
- Yang, W., Gludovatz, B., Zimmermann, E.A., Bale, H.A., Ritchie, R.O., Meyers, M.A., 2013b. Structure and fracture resistance of alligator gar (*Atractosteus spatula*) armored fish scales. *Acta Biomater.* 9 (4), 5876–5889. (April).
- Zhu, D., Barthelat, F., Vernerey, F.J., 2012a. The intricate multiscale mechanical response of natural fish-scale composites, In: Shaofan Li, Xin-Lin Gao. (Eds.), *Handbook of Micromechanics and Nanomechanics*, Pan Stanford Publishing Pte. Ltd., Singapore.
- Zhu, D., Ortega, C.F., Vernerey, F.J., Barthelat, F., 2012b. Structure and mechanical performance of a 'modern' fish scale. *Adv. Eng. Mater.* 14 (4), B185–B194. (April).
- Zhu, D., Szwedciw, L., Vernerey, F., Barthelat, F., 2013. Puncture resistance of the scaled skin from striped bass: collective mechanisms and inspiration for new flexible armor designs. *J. Mech. Behav. Biomed. Mater.* 24, 30–40.